Final report

Marie Curie Intial Training Network Environmental Chemoinformatics

(ITN-ECO)

Modulatory effect of graphene nanoplatelets on pollutant-induced cytochrome P450 1A expression using the PLHC-1 fish cell line

<u>Keywords:</u> GRAPHENE; PAHs/PCBs ; CO-INCUBATIONS; EROD; RT-qPCR; PLHC-1

ITN-ECO Short-term Research Fellow: Paul Boisseaux

Principal Investigator and supervisor: Dr. José Maria Navas

Host institution: Instituto Nacional de Investigación y Technología Agraria y Alimentaria (INIA), Crta. de la Coruna, Km 7.5, 28040 Madrid, Spain

June 2013

Note:

All data represented in this report are confidential and for internal use only. All rights belong to the authors of the work and/or, in case of prior publication of the work, to the publishers. All text, data and images represented in this document must not be made publicly available or reproduced (including making copies, making derivative works, abstracting parts for citation or quotation etc.) without prior permission of the authors and/or the publishers, respectively.

Table of contents

Table of illustrations

AhR: Aryl hydrocarbon Receptor

BkF: Benzo(k)Fluoranthene

βNF: β-Naphtoflavone

CXYG: Carboxylated Graphene

Cyp1a: Cytochrome P450 1A

DMSO: Dimethyl sulfoxide

EC50: concentration that elicits 50% of the assessed effect

EDTA: EthyleneDiamineTetraacetic Acid

EROD: 7-EthoxyResorufin-O-Deethylase

FBS: Fetal Bovine serum

GO: Graphene oxide

MEM: Minimal Essential Medium

PAH: polycyclic aromatic hydrocarbons

PBS: phosphate buffered saline

PCB: polychlorinated biphenyl

REA: Relative EROD Activity

RT-qPCR: Reverse Transcriptase quantitative Polymerization Chain Reaction

SEM: Standard Error of the Mean

Background and context

Nowadays, nanotechnologies hold an important position in R&D with applications covering a wide spectrum. Discoveries of such cutting-edge technologies lead to the necessity to fill the gap of safety issues by assessing the toxicity they may cause for the health and the environment. Due to the extraordinary physico-chemical properties exhibited by nanoparticles, their fate and behavior into the environment and onto the living matter remain uncertain and more insights have to be gained. In 2010, the Nobel Prize in Physics was awarded to Andre Geim and Konstantin Novoselov for the isolation of the graphene nanomaterial from graphite blocks, hence opening the doors for massive industrial application. Graphene is a monolayer of carbon, one atom thick of sp2 hybridized carbons hexagonally arranged. It possesses outstanding properties regarding the stiffness, the weight, the electric velocity and the sorption capacity. The main potential applications are related to sectors as architecture design, electronic devices (transistors), sports (tennis), environment (high yield photovoltaic panels) and medicine (drug-carriers) [1, 2, 3, 4].

In previous studies carried out in the laboratory *Endocrine Disruption and Toxicity of Contaminants*, at the Department of Environment, INIA, it has been observed that two kinds of functionalized graphene, graphene oxide (GO) and carboxylated graphene (CXYG), are internalized into a human hepatoma (HEPG2) cell line after 72 h of exposure. Moreover, they induce dose-dependent oxidative stress and slight but significant cytotoxicity at concentrations as low as 16 µg/ml of culture medium. [5]

The rationale of the present work is based on particular properties and potential applications of graphene nanoplatelets. It has been demonstrated that graphene is a strong surface adsorbent for polycyclic aromatic hydrocarbon (PAHs) molecules. The similarity in the molecular conformation of PAHs and graphene make PAHs easy to adsorb on the inner lattice of graphene rings where π-π stacking stabilize the molecule and *Wan der Waals* interactions being the driving forces [6, 7, 8, 9]. In addition, graphene nanoplatelets have been studied for medicine applications as candidate for drug carriers, able to stick the active compound, transport it through the bloodstream and release the molecule into the target cell. [4]

As a matter of fact, a possible mixture of pollutants and graphene nanoplatelets in a system (*in vitro* or *in vivo*) may modulate the toxicity of these pollutants on the surrounding living matter (e.g. aquatic species). Moreover, the chemical properties of the co-incubated molecule may play a role on the ability of graphene to modulate mechanisms of detoxification in the target cell. More specifically, graphene may reduce the toxicity of a pollutant by adsorbing it and therefore lowering its bioavailability for the cell. But at the same time graphene may increase the toxicity by facilitating the entrance and release of the toxic compound into the cell.

Some pollutants act as ligands of the Aryl hydrocarbons Receptor (AhR). After binding, the receptor undergoes a transformation related with the loosing of some chaperone proteins and the interaction with new proteins and transcription factors and the activated AhR is able to interact with particular regions of the DNA leading to the transcription of dependent genes. One of these genes in fish is this of the cytochrome P4501A (CYP1A). The activity of this cytochrome can be assessed through one of its dependent enzyme activity, as for instance 7-ethoxyresorufin-*O*-deethylase (EROD) activity. Since this work was based on the study of the effects of co-incubations of graphene and CYP1A-inducing pollutants, the measurement of EROD activity appeared to be an insightful endpoint.

Nanoplatelets of two functionalized graphene (GO and CXYG) have been co-incubated with different pollutants in a fish cell line (PLHC-1, *Poecilipsis lucida* hepatoma cells). Three prototypical AhR-agonists were selected: β-naphtoflavone (βNF), benzo(k)fluoranthene (BkF) and polychlorinated biphenyl 169 (PCB169). Care was taken to choose PAH-like molecules with different octanol-water partition coefficient so that insights regarding the chemical properties of the pollutant on the suggested ability of graphene to modulate the toxicity response may be gained. Besides, complementary laboratory assays involving assessment of the aforementioned pathways at the transcriptional level were carried out during this project to verify/complete some hypothesis that arose along with the results.

1. Materials and Methods

   1.1. EROD assays

Chemicals

Cell culture: L-glutamine (200 mM), fetal bovine serum (FBS), penicillin and streptomycin (P/S) (10 000 U/ml / 10 mg/ml), Trypsin EDTA (200 mg/l EDTA, 17000 U trypsin/L), cell culture α-MEM (Alpha Minimum Essential Medium Eagle) media were from Lonza (Barcelona, ES). Phenol red-free Minimum Essential Medium (MEM) and α-MEM were from PAN-Biotech (Aidenbach, DE).

Assay reagents, chemicals and solvents: Ethoxyresorufin (resorufin ethyl ether), resorufin and fluorescamine were sourced from Sigma-Aldrich (Madrid, ES). Acetonitrile was sourced from Sigma-Aldrich (Madrid, ES). High grade purity water (> 18 MΩ cm-1) was obtained from a Milli-Q Element A10 Century (Millipore Iberia, ES).

Dispersion of graphene derivative nanomaterials

Graphene oxide and Carboxylated graphene dispersions (1 mg/ml) were prepared in Millipore water. The samples were ultrasonicated at 37 kHz for 2 h in a bath-type ultrasonic cleaner unit (Elmasonic S 40/(H), Elma). The water in the tank was replaced manually every 15 min with chilled water to prevent heating of the sample (the maximal temperature was 30 ° C).

The resulting oxidized graphene and carboxylated grahene solutions obtained in milliQ water were then centrifuged at 3000 rpm during 30 min in order to remove the biggest particles that may easily sediment over time. Then the concentration was adjusted to 160 µg/mL and 320 µg/mL respectively for oxidized graphene and carboxylated graphene. Concentrations were measured by means of a standard curve obtained by absorbance at 320 nm wavelength.

Routine cell culture

The hepatocellular carcinoma cell line PLHC-1 (derived from topminnow, *Poeciliopsis lucida*) was obtained from the American Type Culture Collection (ATCC) (Manassas, VA, USA). PLHC-1 cells were cultured in 75 cm^2 Cell Star cell culture flasks (Greiner Bio-One GmbH, Frickenhausen, DE) in α-MEM supplemented with 1 % L-glutamine, 1 % P/S and 5 % FBS. The flasks were incubated at 30 ºC in a humidified 5 % CO_2 atmosphere and split prior to reach confluency using PBS/EDTA and trypsin.

Seed of cells and treatments

Cells were seed onto a flat bottom 96-well plate (Greiner bio-One, Frickenhausen, DE) at a density of 50.10^3 cells/well with a final volume of 100 µl/well. The plates were incubated for 24 h at 30 ºC in a humidified 5 % CO_2 atmosphere for the cells to settle down in a monolayer and reach a confluence of approximately 80%. Then, wells were washed twice with PBS and each corresponding exposure medium was added with a final volume of 100 µl per well.
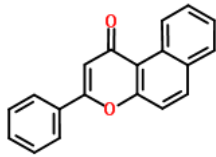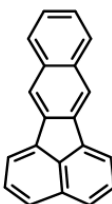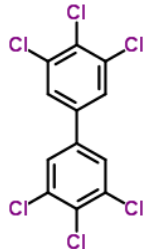
In the CO-INCUBATION assays, the well plates were treated with increasing concentrations of AhR agonists (β-NF: 78 nM – 20 µM, PCB169: 2.4 pM – 625 nM, B(k)F: 5nM – 1.25 µM) alone and in the presence of 4 and 16 µg/ml of GO or CXYG, respectively. Plates were then incubated in the routine cell conditions for 24h and the EROD activity was measured as described in the next section.

In the PRE-INCUBATION assays, plates were firstly pre-treated with CXYG (at 4 and 16 µg/ml) or increasing B(k)F concentration (5nM – 1.25 µM) for 24h in the corresponding cell conditions. Then, the exposure treatment was discarded and cells were washed twice with PBS

pre-warmed at 30°C. Plates were then post-treated with increasing B(k)F concentration (5nM – 1.25 µM) or with CXYG (at 4 and 16 µg/ml), respectively, for another 24h. The EROD activity was measured as described in the next section.

Stock solution of toxicants were previously prepared in DMSO and then diluted in cell medium with a maximal DMSO proportion of 0.1% (v/v). In each experimental batch, vehicle controls contained fixed supplement of 10% of sterile milliQ water (maximal proportion of water added to the cell culture medium with the graphene suspensions) and a maximal proportion of 0.1% of DMSO (v/v). Cells treated with 0.1 % DMSO, 0.1 % DMSO and 4 µg/ml GO/CXYG, and 0.1 % DMSO and 16 µg/ml GO/CXYG served as negative controls, respectively. As additional controls, cells were treated with culture medium alone, 4 µg/ml GO/CXYG and 16 µg/ml GO/CXYG without DMSO, respectively.

Table 1: Chemical properties of the selected AhR agonists

	β-NF	B(k)F	PCB169
Molecular structure			
logP	5.00	6.19	7.56
Polar Surface Area	26.3 Å²	0 Å²	0 Å²
H bond acceptors	2	0	0
H bond donors	0	0	0
Molecular mass	272.1 Da	252.3 Da	360.9 Da

Measurement of cytochrome P450 1A-dependent 7-ethoxyresorufin-O-deethylase (EROD) activity

Following incubation, the exposure medium was aspirated and cells rinsed twice with phenol red-free MEM pre-warmed at 30 °C. Subsequently, 100 µl of 2 µM 7-ethoxyresorufin solution (prepared in phenol red-free MEM pre-warmed to 30ºC) was added to each well and the fluorescence intensity measured using a Tecan Genios microplate reader (Tecan Group Ltd., Männedorf, CH) equipped with a 532 nm excitation and 590 nm emission filter. The fluorescence was read in 10 min intervals, for 30 min. Then, the medium was discarded, the plates washed once with PBS and thereupon frozen using liquid nitrogen. After storage at -20 ºC for at least 1 h, the total protein content in each well was determined by first reconstituting the frozen cell lysate in 75 µl of PBS and then adding 75 µl of fluorescamine (at 0.15 mg/ml) in acetonitrile to each well. Fluorescamine fluorescence was read at 360/450 nm (excitation/emission) using a Tecan Genios microplate reader. EROD activity was calculated by converting resorufin and fluorescamine fluorescence units into amount of substrate (pmol) and amount of protein (mg) per well using a resorufin and albumin standard curve, respectively.

Data analysis for EROD measurements

Since all repetitions showed the same trend (increased sensitivity/potentiation) but variations in the absolute values (EROD activity), for all repetitions the measured EROD activity was first normalized to the maximum response (EROD activity) observed in the respective experiment for the AhR agonist alone (i.e. in absence of GO/CXYG).

Effective concentration 50 (EC50, i.e. the concentration eliciting 50% of the maximal observed effect) was calculated by fitting the data to a logarithmic four parameter function: y=max/[1+(x/EC50) b] + min, (where max is the maximal response observed, b is the slope of the curve and min is the minimal response. For that the Sigmaplot 12 program (Systat Software Inc, CA, USA) was used.

1.2. Transcriptional assays

Seed of cells

The routine cell culture of the PLHC-1 cell line was the same as mentioned above. Cells were seed on a 6-well plate certified nuclease-free and coated with a Nuclon Δ Surface (NUNC, Danmark) at a density of $1.5.10^6$ cells/well with a final volume of 2 ml/well. The well plates were incubated for 24 h at 30 ºC in a humidified 5 % CO_2 atmosphere for the cells to settle down in a monolayer and reach approximately 80% of confluence. Then, wells were washed twice with PBS and each corresponding exposure treatment was added with a final volume of 2 ml/well.

Co-exposure assays

Wells were treated with B(k)F AhR-agonist at 156 nM ± GO/CXYG at 4 or 16 µg/ml for 24h. The corresponding negative control was set up with the same proportion of water (10%) and DMSO vehicle solution (0.01%). After the incubation, the exposure was stopped as described in the section *RNA isolation* (see below).

Pre-exposure assays

The AhR-agonist B(k)F was added for 24h in all wells at a final concentration of 156 nM in α-MEM except for the negative control that contained only α-MEM. Thereafter this pre-exposure step, wells were washed twice with PBS. The negative control and B(k)F control were taken down immediately meanwhile a post-exposure of CXYG at 16 µg/ml was added to the other treatment groups for 2h, 6h and 24h. For each treatment group, a corresponding negative control which consists of α-MEM supplemented with 10% (v/v) of sterile milliQ water was added.

RNA isolation

After finishing an exposure assay, wells were washed twice with PBS. Then, the total RNA isolation was performed using TRI Reagent (Sigma) and the manufacturer's protocol was adapted to the experiment (Life Technologies, USA). The quality of the isolated RNA was assessed by measuring the absorbance of the RNA solution and calculating the A260/A280 ratios using the NanoDrop ND-1000 (NanoDrop Technologies Inc., DE, USA).

Selection of primers

The sequences of the forward and reverse primers used to amplify the *cyp1A* gene in this PLHC-1 cell line was chosen from available literature to conform with different criteria. Primers 5'-GCATTTGGCGTGCTCGAAGAAA-3' and 5'-TTGCAGATGTGTGCTCCTCCAACA-3' were selected as forward and reverse primers, respectively. The product amplified was of 109 bp [Poeciliopsis lucida cyp1a mRNA, ACCESSION JX270831, Della Torre,C. and Corsi,I].

The *ahr2* and *β-actin* were designed on the PubMed website using the "Primer-BLAST" tool. Regarding the *ahr2* primers, the forward and reverse primers sequences used were respectively 5'-CTCTGTTTGCCATCGCTGTG-3' and 5'-CCCACACTTCAGGTCGAACA-3'. The product amplified was of 101 bp. Regarding *β-actin primers,* the forward and reverse sequences used were respectively 5'-TTGGCAACGAGAGGTTCCG-3' and 5'-AGGCGTCCTGAGGTATGGTT-3'. The product amplified was of 71 bp.

Single-step reverse transcriptase – quantitative polymerization chain reaction (RT-qPCR)

RT-qPCR was carried out using the one-step iScript RT-qPCR kit with SYBR Green (BIO-RAD, CA, USA) and the manufacturer's instructions were adapted to the assay. The thermal cycling conditions were 10 min at 50 °C for the reverse transcription, 5 min at 95 ºC to inactivate the reverse transcriptase, and 35 cycles at 95°C for 15 s, 55 °C for 30 s and 72 ºC for 1 min. Then the melting curve was set up from 55°C to 95 °C by increments of 0.5 °C.

Among the batch of primers used within an assay, the lowest Tm was of 55.2 ºC, corresponding to the reverse primers of *ahr*. Therefore, annealing temperature was set up at 55ºC to optimize the annealing specificity of primers with their target sequence and avoid unspecific annealing.

All PCR reactions were performed in a Line-Gene K System (BIOER Technology, Hangzhou, China) and in duplicate on a 96 well low-profile PCR plate (VWR, USA) with a final volume of 20 µl per well. The *β-actin* was chosen as an internal control (housekeeping gene, i.e. a gene whose expression is not altered in the cells by the treatments) to normalize the expression levels of the target genes. Results of qPCR were finally represented as $2^{-\Delta\Delta Ct}$ values, where Ct was defined as the threshold cycle number at which product is first detected by fluorescence in a phase of exponential growth. The Ct value of the target gene was normalized to the Ct value of *β-actin* of the corresponding treatment and then expressed as time-fold compared to the B(k)F treatment (see below). The data acquired and used for further calculations were generated with the baseline and threshold values that were automatically set up by the LineGene software.

$\Delta Ct_{\text{target gene, treatment A}} = [Ct\ (\textit{target gen}) - Ct\ (\textit{β-actin})]_{\text{treatment A}}$

$\Delta\Delta Ct_{\text{target gene, treatment A}} = \Delta Ct\ (\textit{target gene}, \text{treatment A}) - \Delta Ct\ (\textit{target gene}, \text{BkF treatment})$

The statistical analysis and the graphs were performed with the Sigmaplot 12 software. Bars and error bars represent the mean and standard error of the mean (SEM) of three independent experiments. Statistically significant differences among the results with respect to the B(k)F group were tested by running a one-way repeated measures ANOVA followed by Dunnet as a Post Hoc Test. Statistically significant differences were considered for $p < 0.05$.

2. Results and discussion

Remark: In this report, all the data acquired during the fellowship are not shown in order to simplify the lecture. For instance, in co-incubation assays, the results regarding the carboxylated graphene are not presented but the trends observed were closely similar to the graphene oxide.

2.1. Co-incubation of graphene oxide and selected AhR agonists

In all cases, co-incubation with graphene derivatives led to an increase of the toxicity with respect to the toxicity caused by the AhR agonist alone (Fig. 1). To reach a relative EROD activity (REA) of 50%, the concentration of agonist has to be inversely proportional to the concentration of co-incubated graphene oxide (Table 2).

Although the shift for PCB169+GO 4 µg/ml is really slight, each treatment group (β-NF, PCB169 and B(k)F) elicits significant GO dose-dependent increase of REA. However, the trend for the maximal value differs among the treatment groups. Regarding the β-NF treatments, the three curves reach the same maximum REA of 100% at 10 µM. The PCB169 graph displays three curves reaching a plateau at 0.039 µM but with REA values of approximately 100, 120 and 150% respectively for PCB169, PCB169+GO 4 µg/ml and PCB169+GO 16 µg/ml treatments. Similarly, the BkF-GO 16µg/ml curve hits a high at 150% of REA, whereas the BkF+GO 4 µg/ml is at 130% and the BkF treatment is at 100%. Thus, the βNF graph indicates a dose-dependent increase of potency in co-incubated systems, meanwhile the PCB169 and BkF graphs indicate not only a dose-dependent increase of potency but also a dose-dependent increment of REA maximal amplitude.

The trend previously described at the enzymatic activity level is equally found at the transcriptional level. Indeed, the histogram (Fig. 2) shows that at a constant BkF concentration, a GO dose-dependent increase of relative *cyp1A* mRNA is observed. For instance, at 156 nM of BkF, the *cyp1A* mRNA levels are approximately 3.75 times higher when co-incubated with GO 16 µg/ml.

Table 2: Calculations for the analysis of EROD co-incubation assays

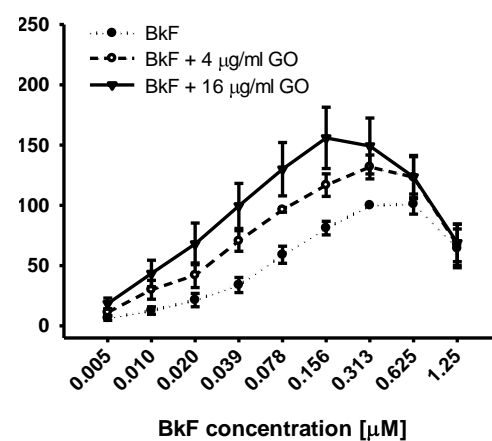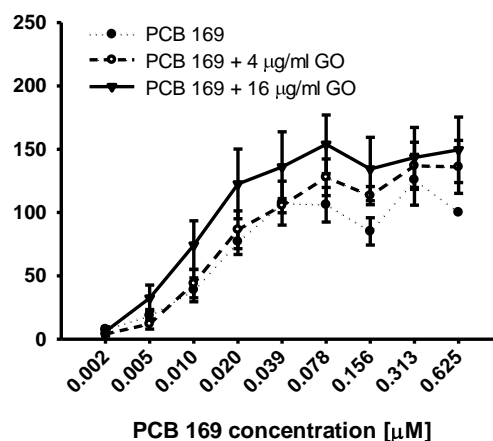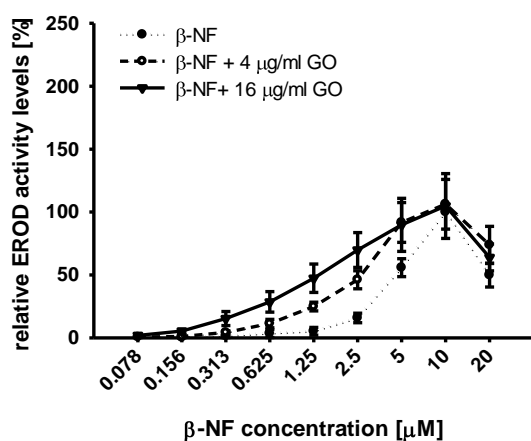| Treatment groups	EC50 of respective AhR-agonist alone and corresponding concentration for co-incubated groups [µM]	Increase in potency $EC50_{single}/EC_{co-exposure}$	REA maximal amplitude [%]
ßNF	3.2844	1	100
ßNF + 4 µg/ml GO	2.7354	1.2	118.9
ßNF + 16 µg/ml GO	1.9837	1.65	124.4
BkF	0.0601	1	100
BkF+ 4 µg/ml GO	0.0435	1.38	115.7
BkF+ 16 µg/ml GO	0.0402	1.49	121.25
PCB169	0.0642	1	100
PCB169 + 4 µg/ml GO	0.0607	1.06	109.9
PCB169 + 16 µg/ml GO	0.0371	1.73	142.0

Figure 1: GO nanoplatelet-dependent changes in β-NF, BkF and PCB169-induced EROD activity levels

PLHC-1 cells were exposed to increasing concentrations of β-NF, B(k)F and PCB169 (β-NF: 0.078 – 20 µM; BkF: 0.01 – 2.5 µM; PCB169: 0.002 – 0.625 µM) alone and together with 4 and 16 µg/ml GO, respectively. The data points and error bars represent the mean and standard error of the mean (SEM) of three (β-NF) or four (BkF and PCB 169) independent experiments. The presence of GO potentiated the response induced by the different AhR agonists.
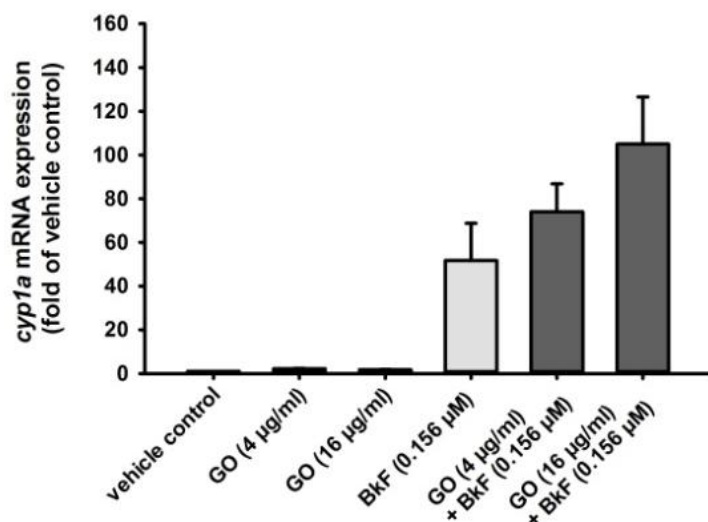
Figure 2: GO -dependent increase of Cyp1A mRNA expression levels

Relative *cyp1A* mRNA expression levels in PLHC-1 cells co-exposed to BkF (0.156μM) and GO (4 and 16 μg/ml) for 24 h. *cyp1A* mRNA expression levels are represented as fold expression of *cyp1A* mRNA levels measured in the vehicle control. Bars and error bars represent the mean and standard error of the mean (SEM) of three independent experiments.

The results raise different hypothesis to explain the trends observed. First of all, it may be possible that graphene transports the toxic agonist from the extracellular matrix into the cytosol. Therefore, the intracellular concentration of agonist is higher in co-incubated systems (before reaching the maximal response in the case of βNF) where passive diffusion and "graphene carriage" entrances co-exist. When the agonist is not co-incubated with graphene, only passive diffusion would occur. In the case of βNF, the three curves reach the same maximal response at 10 μM. The octanol-water partition coefficient (log P) of βNF is 5 which corresponds to a lipophilic chemical that goes easily through the phospholipidic bilayer membrane and accumulates into the intracellular compartment via passive diffusion. However, in the case of PCB169 and BkF, the three internal curves of corresponding graph reach a different maximal amplitude which is GO dose-dependent. In such cases, the log P values are higher, respectively 6.19 and 7.56 for the PCB169 and the BkF. When 6<log P<8, the superlipophilic chemical tends to have a smaller bioconcentration factor than when 4<log P<6 [10, 11]. Therefore, it can be hypothesized that in such situations the passive diffusion of the agonist is smaller and not efficient enough to break even the increment of REA generated by the transportation of agonist by graphene nanoplatelets. Furthermore, a parallel study carried out in the laboratory showed that GO is internalized into the intracelullar compartment in this PLHC-1 cell line which comfort this hypothesis of pollutant carriage by graphene.

Secondly, the graphene may damage the membrane facilitating the entrance of isolated agonist from the extracellular matrix into the intracellular compartment. This is comforted by previous cytotoxicity studies carried out in the laboratory reporting that GO/CXYG nanoplatelets exert, although slightly, a dose-dependent cytotoxicity and decrease of the plasma membrane integrity at concentrations as low as 16 µg/ml [5].

Finally, a third possibility would be that graphene is metabolized and the resulting metabolites are able to retroactivate the AhR-CYP1A pathway. Since the graphene is a monolayer of hexagonally arranged carbon atoms, it might be viewed as a superstructure of PAHs all covalently bonded together. Therefore, if the EROD activity, initially induced by AhR-agonists, metabolizes the graphene, then some metabolites may acquire the prototypical steric conformation of PAHs able to activate the AhR.

2.2. Complementary results: pre-incubation assays of carboxylated graphene and benzo(k)fluoranthene

A

Pre-incubation of benzo(k)fluoranthene (BkF) for 24h
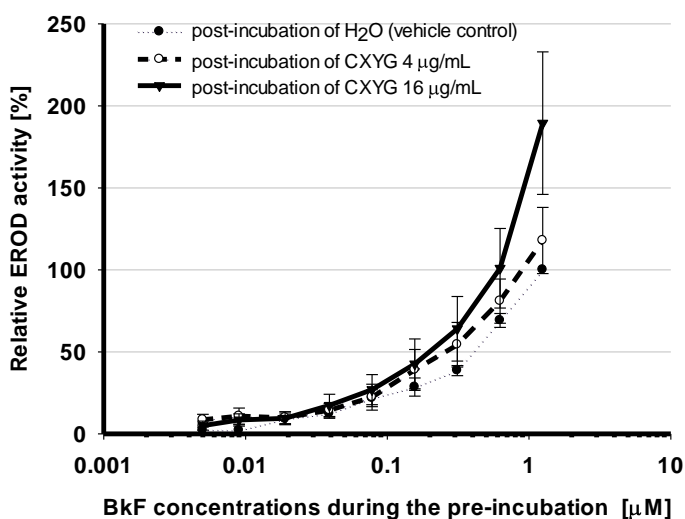**Post-incubation of carboxylated graphene (CXYG) for 24h**

**Figure 3: CXYG nanoplatelet-dependent changes in BkF-induced EROD activity levels**

A) PLHC-1 cells were exposed to increasing concentrations of BkF for 24h, which was then discarded and replaced by CXYG (4 and 16 µg/ml) for another 24h.
B) PLHC-1 cells were exposed to CXYG (4 and 16 µg/ml) for 24h, which was then discarded and replaced by increasing concentrations of BkF for 24h for another 24h.
The data points and error bars represent the mean and standard error of the mean (SEM) of three independent experiments. The presence of CXYG resulted in a potentiation of the response induced by the different AhR agonists.

B

Pre-incubation of carboxylated graphene (CXYG) for 24h
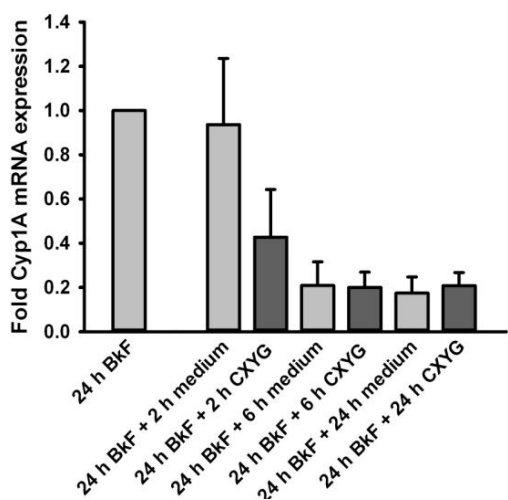**Post-incubation of benzo(k)fluoranthene (BkF) for 24h**
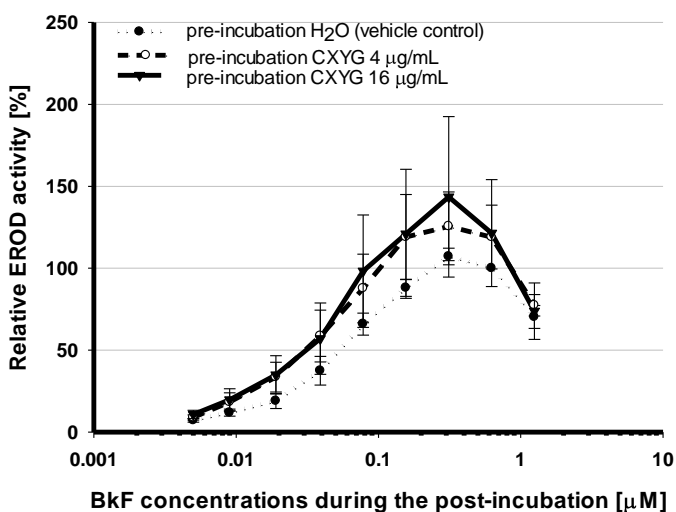
Figure 4: CXYG-independent loss of *cyp1A* mRNA expression levels in post-BkF incubation situation

PLHC-1 cells pre-incubated with BkF for 24 h were exposed to 16 µg/ml CXYG for 2, 6 and 24 h. *cyp1A* mRNA expression is represented as fold expression level of that measured after pre-incubation with BkF. Bars and error bars represent the mean and standard error of the mean (SEM) of three independent experiments. No recovery over time of the Cyp1A mRNA levels is observed after post-addition of CXYG 16 µg/ml.

When cells were pre-exposed to B(k)F and thereafter incubated with CXYG alone, a decrease in the B(k)F concentrations leading to an equal EROD activity (i.e. a left shift of the REA when represented graphically) was observed. This was simultaneous to an increase in the maximal values of REA: at B(k)F 1.25 µM, REA reached approximately 190% in CXYG 16 µg/ml group meanwhile it reaches 100% in control group not post-CXYG treated (Fig 3A). So far, these results cannot reject the metabolites hypothesis. Now, paying attention to the results at the transcriptional level, results suggest a different mechanism. The histogram (Fig. 4) states a decrease of *cyp1A mRNA* quantified when taking off the agonist and adding the CXYG. Then, the *cyp1A* mRNA level decreases over time until stabilize at a basal level. These results reject the hypothesis of CXYG metabolites asserting a retroactivation of the AhR-mediated Cyp1A pathway. In fact, in such case a recovery of the *cyp1a mRNA* levels would have been observed after 5 and 24h because of the metabolization of graphene and the further retroactivation.

In the second pre-incubation assay, cells were pre-exposed to CXYG and thereafter incubated with different concentrations of BkF. A similar pattern as in the corresponding co-incubation assay is obtained (Fig. 3B). In this experimental design, the agonist and the nanoplatelets are not incubated at the same time. Therefore, the graphene-carriage is avoided and the observed modulatory effect would result from the pre-treatment of CXYG nanoplatelets that damaged/destabilized the outer membrane of the cell and thereupon facilitated the entrance of the agonist during the post-incubation.

18

The graphene nanoplatelets lead to an increase in the dose-dependent induction of EROD activity triggered by the selected pollutants in the PLHC-1 cell line. This trend is observed not only with functionalized grapheme oxide but also with carboxylated graphene. This effect is equally observed at the transcriptional level. It appears very unlikely that graphene metabolites are involved in the observed modulation of EROD activity. Rather, graphene nanoplatelets would adsorb and transport the pollutant into the cell and/or destabilize the plasma membrane which would facilitate the entrance of the toxic compound into the cytosolic compartment. The combination of both mechanisms is likely to happen. Besides, they corroborate previous studies claiming that graphene is internalized and damages the outer membrane in this PLHC-1 fish cell line.

Acknowledgements

References

[1]: http://sensingarchitecture.com/6779/uses-of-nanotechnology-for-architectural-design-the-graphene-skin/

[2]: Development of graphene transistor with new operating principle, http://phys.org/news/2013-02-graphene-transistor-principle.html

[3]: Xiaochang Miao *et al.*, High efficiency graphene solar cells by chemical doping, Nano Letters, (2012), DOI:10.1021/nl204414u

[4]: Xiaoying Yang *et al.*, Multi-functionalized graphene oxide based anticancer drug-carrier with dual-targeting function and pyH-sensitivity, J. Mater. Chem., (2011), DOI: 10.1039/C0JM02494E

[5]: T. Lammel, P. Boisseaux, ML Fernández-Cruz, JM Navas Antón, Internalization and cytotoxicity of graphene oxide and carboxyl graphene 1 nanoplatelets in the human hepatocellular carcinoma cell line Hep G2 2, Particle and fibers, (2013), *[submitted and accepted]*

[6]: Ming Zhang *et al*., Synthesis, characterization and environmental implications of graphene-coated biochar, Science of the total environment, (2012), DOI: 10.1016/j.scitotenv.2012.07.038

[7]: Svetla D Chakarova-Käck *et al.*, Binding of polycyclic aromatic hydrocarbons and graphene dimers in density functional theory, New Journal of Physics, DOI: 10.1088/1367-2630/12/013017

[8] Thien Tran-Duc and Ngamta Thamwattana, Modelling Carbon nanostructures for filtering and adsorbing polycyclic aromatic hydrocarbons, Journal of computational and theorical nanoscience, (2011), DOI: 10.1166/jctn.2011.1928

[9]: Hong Zhang *et al.*, Evaluation of sulfonated graphene sheets as sorbent for micro-solid-phase extraction combined with gas chromatography-mass spectrometry, Journal of Chromatography A, (2012), DOI: 10.1016/j.chroma.2012.02.020

[10]: Martin Müller, Monika Nendza, Literature Study: Effects of Molecular Size and Lipid Solubility on Bioaccumulation Potential, (2007), Fraunhofer, Institut Molekularbiologie und Angewandte Oekologie

[11]: Harald J. Geyer *et al.*, Bioconcentration of superlipophilic persistent chemicals, Environmental Science and Pollution Research , (1994), DOI: 10.1007/BF02986510